FUEL CYCLE ANALYSIS OF A SUBCRITICAL FAST HELIUM-COOLED TRANSMUTATION REACTOR WITH A FUSION NEUTRON SOURCE

RADIOACTIVE WASTE MANAGEMENT AND DISPOSAL

KEYWORDS: *transmutation, fuel cycle*

J. W. MADDOX* and W. M. STACEY† *Georgia Institute of Technology*
Nuclear and Radiological Engineering Program, Atlanta, Georgia 30332-0425

Received May 5, 2006
Accepted for Publication August 21, 2006

Geologic repositories for the long-term storage of spent nuclear fuel (SNF) are limited in their capacity by the amount of decay heat emitted by the SNF. The largest long-term contribution to this decay heat comes from the transuranics (TRUs), the destruction of which could increase storage capacity by a factor of at least 10. A design concept for a subcritical gas-cooled fast transmutation reactor (GCFTR) fueled with TRUs from SNF is being developed. This paper presents the results of analyses of several GCFTR fuel cycle scenarios that have a deep-burn (>90% burnup of the TRU fuel) primary objective and a secondary objective of avoiding reprocessing of the TRU fuel if possible.

I. INTRODUCTION

Five decades of commercial nuclear power production in the United States have created ~50 000 tonnes of spent nuclear fuel (SNF) distributed at numerous locations throughout the country—a number that will continue to increase by 2000 tonnes/yr at the present level of nuclear power production.[1] To provide a permanent repository for spent fuel from commercial nuclear reactors and government sources [U.S. Department of Defense and U.S. Department of Energy (DOE)], the Yucca Mountain Project was undertaken to create a high-level waste repository (HLWR) with a capacity of 70 000 tonnes. At the current rate of SNF production, a new storage facility comparable to the Yucca Mountain facility would be required every 34 yr (Ref. 2).

*Current address: AREVA, Lynchburg, Virginia
†E-mail: weston.stacey@nre.gatech.edu

Repository capacity is determined primarily by decay heating, which for SNF after several hundred years (by which time the short-lived fission product radioactivity decays substantially) is primarily due to the remaining long-lived transuranics (TRUs). If the TRU content of SNF could be reduced, the long-term decay heat would be reduced, the repository capacity could be increased, and the time until a new repository following Yucca Mountain is needed would be lengthened. Since the most abundant SNF TRU, plutonium, may also be used in nuclear weapons, TRU reduction in SNF also constitutes an increase in proliferation resistance as it destroys any incentive for intrusion and diversion. The only known method of destruction of the TRUs is via neutron fission, the energy release from which could be used to generate electricity.

There may be both criticality and safety advantages to subcritical operation of transmutation reactors. Subcritical operation with a neutron source rate that can be increased to compensate for the negative reactivity caused by fissile depletion and fission product buildup should be advantageous in obtaining deep burnup of the TRUs, while reducing the need for reprocessing to remove fission products and add fresh TRUs. The dominance of plutonium in the TRU content of the SNF indicates that a TRU fuel extracted from SNF will have a smaller delayed neutron fraction [$\beta = 0.020$ for ^{239}Pu, $\beta = 0.064$ for ^{235}U (Ref. 3)] than equivalent ^{235}U fuel. In a critical reactor, the margin of safety for accidental reactivity insertions (i.e., the value of reactivity for which a prompt critical excursion occurs) is β, but in a reactor operating subcritical by $\Delta k = 1 - k_{eff}$, the margin of safety is $\beta + \Delta k$, which can be considerably larger.

Research interest in SNF transmutation has focused on both accelerator-driven systems[1,4–8] and, to a much lesser extent, on fusion-driven systems.[9–19] The Accelerator Transmutation of Waste (ATW) Roadmap, requested by the U.S. Congress in 1999, evaluated the status and potential of, and proposed a path of development for,

subcritical, accelerator-driven transmutation systems. This study concluded that the use of an ATW system to transmute light water reactor (LWR) SNF could destroy 99.9% of its TRU content and reduce the radiation dose of a repository such as the proposed facility at Yucca Mountain by a factor of 10 (Ref. 1).

The possible advantage of using a fusion neutron source, instead of an accelerator neutron source, was suggested by Parish and Davidson,[9] who determined in a study evaluating neutron sources for fission product transmutation that accelerator-driven systems will likely consume a great deal of energy, while fusion-driven transmutation can potentially produce a great deal of energy. This same general conclusion was found in subsequent studies of systems for the transmutation of TRUs by Stacey[15] and Jassby and Schmidt.[20] Because the reactor will provide most of the transmutation neutrons, and the neutron source need only provide enough neutrons to maintain the chain reaction, the performance requirements are less demanding than for a fusion device intended for power production and are within the ken of the current tokamak operational database, indicating that such a tokamak is practicable subject to availability requirements of at least 50% (Refs. 15 and 17). The fusion neutron source has another advantage over the accelerator-spallation neutron source because the distribution of the source over a large volume results in less demanding heat removal requirements and radiation damage limits.[16,17]

Several exploratory studies of transmutation of SNF with subcritical reactors driven by fusion neutron sources have been performed. Peng and Cheng[11] investigated the electricity-generating capacity of a fusion-driven transmutation system to determine the practicality of small fusion devices employed to transmute nuclear waste in high epithermal flux regions. Cheng and Cerbone[12] analyzed and compared two tokamak-based transmutation reactors: (a) minor actinide (MA) fueled and (b) "Pu assisted" (Pu + MA fuel), which they determined could operate at $P_{fus} = 200$ MW, $k_{eff} \sim 0.8$ and $P_{fus} = 75$ MW, $k_{eff} \sim 0.9$, respectively. Stacey et al.[19] developed a metal fuel, liquid-metal–cooled, subcritical transmutation of waste reactor driven by a tokamak neutron source with a four-batch fuel cycle that was predicted to achieve a discharge burnup of 25% per cycle with a cycle time of 623 days, P_{fusion}^{EOC} of 150 MW, and k_{eff}^{BOC} of 0.95. Hoffman and Stacey[2] examined both ATW and fusion-driven systems and found that repeated recycling of TRUs through fast transmutation reactors would substantially reduce repository heat removal requirements and increase proliferation resistance.

The use of the coated trimaterial isotropic (TRISO) particle adds an additional level of containment that introduces the possibility of deep burn of TRU fuel without reprocessing. This is because the TRISO layers form a corrosion-resistant pressure vessel that serves to contain the fission products released during irradiation and for millions of years afterward in storage, in wet or dry conditions,[21,22] thus making the TRISO particle an attractive choice for deep-burn transmutation and long-term storage provided the particles can withstand the high irradiation levels concomitant to deep burn. Rodriguez et al.[22] investigated a deep-burn, thermal spectrum, modular, helium-cooled, critical reactor (modular helium reactor) fueled with the TRU component of LWR SNF in TRISO particles. Very high burnups (>65% Pu, >95% ^{239}Pu) of Pu-oxide kernels were predicted without particle failure. By comparison, experimental burnups of 79% of fertile and fissile content at temperatures of 1030 to 1240°C and fast fluences of 3.8×10^{21} n/cm^2 were reported in a study comparing German and U.S. fuel TRISO performance.[23]

Transuranic TRISO fuel has been used in a series of conceptual designs of gas-cooled fast transmutation reactors (GCFTRs) driven by a fusion neutron source.[24,25] Both TRISO and bi-isotropic (BISO) fuel particles were examined, using SiC and Zircaloy-4 fuel matrices, respectively. This series of GCFTR designs and the previous metal-fueled fast transmutation reactor designs are summarized by Stacey et al.,[18] and Stacey[17] has discussed how the development of the tokamak fusion neutron source would fit into the DOE fusion program. The present work is based on the second of these designs, GCFTR-2 (Ref. 25). Several fuel cycle scenarios are analyzed to explore how the GCFTR-2 design can achieve >90% burnup of TRUs, with an emphasis on examining the possibility of doing so without reprocessing.

Section II briefly summarizes the GCFTR-2 reactor design and gives an overview of fuel production. Section III describes the computational methodology employed to model the design and simulate the fuel cycle. In Sec. IV, the fuel cycle scenarios analyzed in this work are described. Section V discusses the results of the fuel cycle analyses in terms of transmutation performance. Section VI presents a summary and conclusions of the work.

II. REACTOR DESIGN

The reactor design used in this study and described in this section is based on the GCFTR-2 (Ref. 25), the salient parameters of which are given in Table I. The central part of the reactor consists of a toroidal plasma chamber outboard of which is the annular reactor core (Fig. 1). Surrounding the plasma chamber is the first wall, which is composed of ferritic steel, with HT9 taken as a representative example. Both the first wall and reactor core are surrounded by the reflector, which serves to return escaping neutrons to the reactor and to the lithium-containing regions to breed tritium. The reflector consists of HT9 and a solid tritium breeder, Li_2O. The tritium produced in the reflector is removed via an online helium purge and is used to fuel the D-T fusion reaction.

TABLE I

GCFTR Parameters

Parameters and Materials	Values
Reactor core	
Annular dimensions	R_{in} = 4.84 m, R_{out} = 5.96 m, H = 3 m
Fuel/He/structure (vol%)	59.5/30/10.5
Fuel element	TRISO particles in SiC matrix, pin d = 1.34 cm
TRU coated particle diameter	660 μm
TRU-oxide fuel volume fraction	60%
TRU fuel mass	35 tonnes
Maximum k_{eff}	0.95
Clad/structural materials	Zircaloy-4/HT-9
Fission power	3000 MW(thermal)
Reflector	
HT9/He/Li_2O (vol%)	Various
Thickness	15 cm
Shield	
W/B_4C/He (vol%)	40/40/20
Thickness	61 cm
Fusion source	
Maximum power, P_{fus}	200 MW

Surrounding the reflector is a shield composed of boron carbide and tungsten, which serves to protect the toroidal field coils from high-energy neutrons and gamma radiation, respectively. The vacuum vessel, composed of HT9, encases the shield and seals the reactor and plasma chamber from the outside environment. The magnets, depicted in Fig. 1 as loops, are based on the ITER design.[25] The core, first wall, magnets, central solenoid, reflector, and shield are all cooled with helium. For greater detail, see Refs. 24 and 25.

The processing of the TRISO fuel particle designed in the GCFTR (Ref. 24) and GCFTR-2 (Ref. 25) studies and used for the present analysis begins with the four-part di-isodecylphosphoric acid partitioning process[25] in which the TRU content of the LWR SNF (Ref. 26) is extracted. Estimated recovery percentages for the TRUs using this process are 99.85% for Np and Pu and 99.97% for Am and Cm with negligible retention of lanthanides and uranium,[25] which is modeled here as perfect separation of fission products, lanthanides, and uranium from the TRUs and TRU recovery with the above-mentioned efficiency. Subsequent to separation, the TRUs are oxidized in a calcination process, blended and homogenized[24] to form the TRISO kernel. After kernel creation, a chemical vapor infiltration process successively deposits the outer layers of the TRISO particle.[25] The resulting fuel kernel composition is shown in Table II.

The TRISO fuel particle design differs from the standard thermal reactor particle design in two respects: (a) The fuel kernel contains pure fissionable (in a fast spectrum) TRU rather than a mixture of fissionable and nonfissionable isotopes and (b) the design is changed to accommodate the greater fast neutron fluence. Operation with a pure TRU fuel to achieve a sizable TRU concentration with coated particle fuel is allowed because of the large reactivity margin to prompt critical provided by subcritical operation.

Each TRISO particle is ~660 μm in diameter and consists of a TRU-oxide kernel 300 μm in diameter surrounded successively by (a) a ZrC buffer region of 100-μm thickness, (b) an inner pyrocarbon layer of 20-μm thickness, (c) a SiC layer of 25-μm thickness, and (d) an outer pyrocarbon layer of 35-μm thickness.[25]

The buffer is 50% void, which allows for the expansion of fission product gases and free oxygen and serves as a shock absorber for the recoiling fission products. Zirconium carbide was used rather than carbon because the Zr acts as an oxygen getter, resulting in a reduced oxygen partial pressure on the inner pyrocarbon layer.[24]

The inner pyrocarbon layer, while providing some structural support, is primarily a means to protect the SiC layer from contact with chemicals employed in the deposition of the buffer layer.

The primary structural support is the SiC layer, which can withstand a maximum pressure of 345 MPa (Ref. 24). Since internal gas pressure is 160 MPa at 90% Fissions Initial heavy Metal Atom (FIMA) and 180 MPa at 99%

TABLE II

TRISO TRU Fuel Kernel Data

Isotope	TRU Composition (10^{24}atoms/cm^3)	Oxide Form	Oxide Melting Point (°C)	Oxide Density (g/cm^3)
^{237}Np	1.06508E−03[a]	$^{237}NpO_2$	2510	11.10
^{238}Pu	3.04308E−04	$^{238}Pu_2O_3$	2085	10.50
^{239}Pu	1.31692E−02	$^{239}Pu_2O_3$	2085	10.50
^{240}Pu	5.17324E−03	$^{240}Pu_2O_3$	2085	10.50
^{241}Pu	9.39158E−04	$^{241}Pu_2O_3$	2085	10.50
^{242}Pu	1.12804E−03	$^{242}Pu_2O_3$	2085	10.50
^{244}Pu	3.82484E−08	$^{244}Pu_2O_3$	2085	10.50
^{241}Am	2.22727E−03	$^{241}Am_2O_3$	2190	11.77
^{242m}Am	1.61267E−06	$^{242m}Am_2O_3$	2190	11.77
^{243}Am	2.46366E−04	$^{243}Am_2O_3$	2190	11.77
^{242}Cm	4.22866E−09	$^{242}Cm_2O_3$	2225	11.85
^{243}Cm	4.27069E−07	$^{243}Cm_2O_3$	2225	11.85
^{244}Cm	2.77358E−05	$^{244}Cm_2O_3$	2225	11.85
^{245}Cm	2.98895E−06	$^{245}Cm_2O_3$	2225	11.85
^{246}Cm	2.36385E−07	$^{246}Cm_2O_3$	2225	11.85
^{247}Cm	2.38486E−09	$^{247}Cm_2O_3$	2225	11.85

[a]Read as 1.06508×10^{-3}.

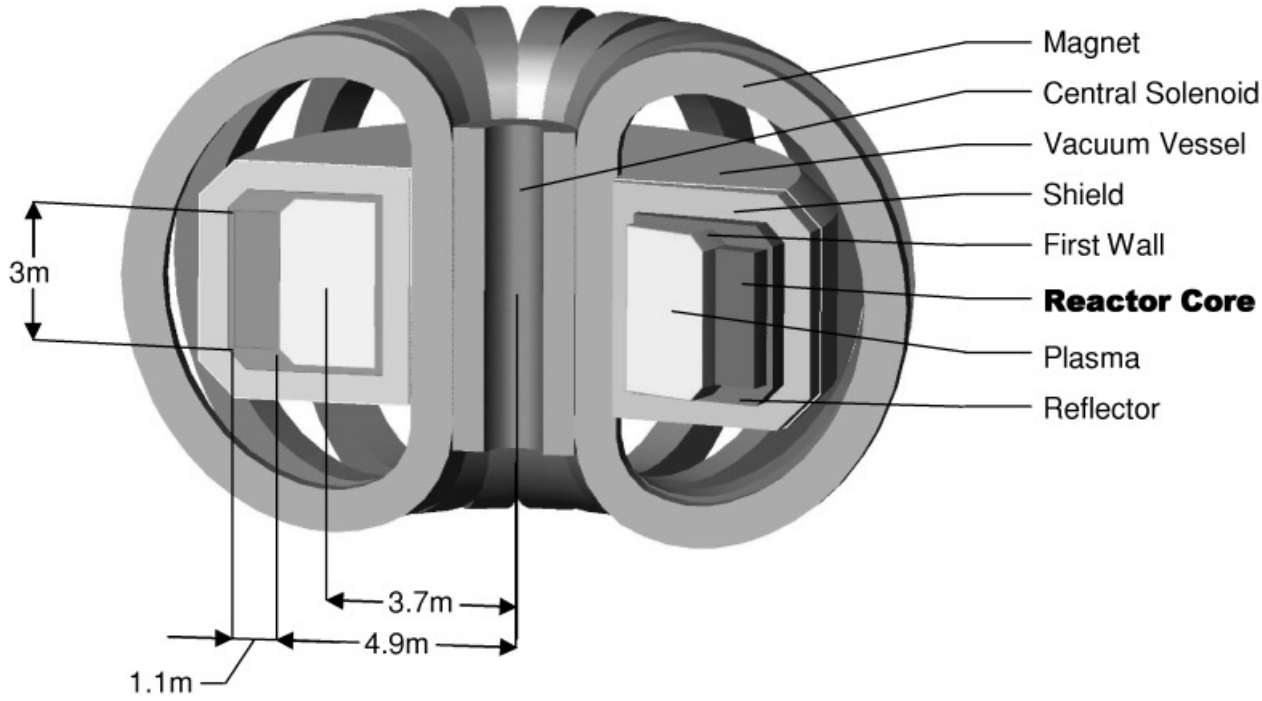

Fig. 1. Schematic of the GCFTR-2.

FIMA (at nominal fuel centerline temperatures[24]), particle failure due solely to fission gas and oxygen pressure is unlikely.

In the event of loss of coolant flow, it is envisioned that decay heat would be removed by radiative heat transfer from the fuel pins to the surrounding reflector and shield. Calculations[25,26] of radiative decay heat removal under complete loss-of-coolant-accident (LOCA) conditions indicate that emergency core cooling would be needed for 1 h or less early in the accident in order to avoid melting of the cladding. It was calculated[26] that a pressure-activated toroidal helium accumulator located above or below the core could maintain the cladding temperature below the melting point and provide for passive safety against the LOCA.

III. FUEL CYCLE ANALYSIS METHODOLOGY

Fuel cycle calculations were performed[27] using the REBUS-3 fuel cycle modeling and depletion code.[28] Transport calculations were performed with the TWODANT two-dimensional, discrete ordinates, flux distribution code[29] using an S_4 approximation. Region-dependent cross sections were generated using MCC-2 (Ref. 30) with a 34-group structure from 14 MeV to thermal using the ENDF-B/V cross-section library and beginning of cycle (BOC) number densities[a] for each core material at the operating temperatures. The core temperature, core coolant, and core structure were 750, 660, and 700 K, respectively, and all other reactor components were at 600 K. The coolant temperature for a given region was 50 K less than the temperature of the given region.

The geometry of the reactor was modeled by REBUS-3 as described in Ref. 27. It was modeled in *R-Z* geometry, which means that it is expressed in terms of radial and axial dimensions relative to a central axis and reactor midplane, respectively. Only the upper half of the reactor was modeled to take advantage of its symmetry about the midplane. It is modeled as toroidally symmetric.

The core was divided into 25 regions (5 radial core regions, each with 5 axial subdivisions of equal height; see Ref. 27). The widths of the five core regions were adjusted to equalize the volumes, which allowed for a given batch to be moved from one core region to the next without a change in fuel density. The number densities were homogenized within each of the 25 regions.

[a]For the purpose of generating cross sections, fission product concentrations were approximated at 50% of their discharge density as indicated by the equilibrium TRU single-pass burnup (i.e., an equilibrium cycle with a 20% single-pass burnup would be modeled with a fission product content corresponding to a 10% burnup in all core regions).

Depletion was modeled only for the actinides. Fission products were modeled as a single lumped species. Neither the fission products in the core nor the lithium in the reflectors were depleted.

Four different fuel shuffling schemes, or paths, were used for the four scenarios (scenario A, B, C, and D described in Sec. IV) developed in this study (Fig. 2). The numbers below the core designate the core region, while the numbers in the core itself indicate the sequence each batch follows through the core. Scenario A used all four paths. Scenarios B, C, and D used path 1.

The fuel paths are directions for how fuel moves through the reactor in successive burn cycles in a five-batch fuel cycle. For example, a fresh batch of fuel in a five-batch core may start in region 1 and move to region 2, then 3, then 4, and finally 5, and then it is discharged. This is path 1 of Fig. 2. Another path is the reverse: A batch starts in region 5; then moves to 4, 3, 2, and finally 1; and then it is discharged. This is path 4 of Fig. 2. Batches using path 2 begin in region 4 and move to regions 3, then 5, then 2, and finally 1, and then the fuel is discharged. Batches using path 3 follow the reverse sequence. They begin in region 1; then move to 2, 5, 3, and finally 4; and then they are discharged. Paths 2 and 3 arose from the observation that for a homogeneous core composition, the magnitude of the flux is highest in region 4; the next highest flux occurs in region 3, then 5, 2, and 1. Thus, path 2 matches burn rank to flux rank. This was done to maximize the cycle time. The opposite of this, path 3, was used to minimize the power peaking.

REBUS-3 models the fuel paths by specifying the sequence of core regions in which the fuel batches burn. It also models the between-cycle downtime during which the batches are moved to the next core region in the sequence and fresh fuel is added. A downtime of 30 days for batch shuffling was used.

After discharge, the fuel is not immediately processed because it is highly radioactive. It is cooled for a time to allow the radioactivity to decrease. A cooling time of 730.5 days was modeled.

All fuel cycle calculations were for "equilibrium" fuel cycles. An equilibrium fuel cycle is a steady-state fuel cycle where the composition of the fuel charged to and discharged from the core, as well as the core composition itself, have all become constant because of a large number of executions of the fuel cycle. All core parameters at BOC and end of cycle (EOC) have become steady state. This is in contradistinction to a start-up core that will necessarily have different core enrichment and performance parameters from cycle to cycle that will change as new core batches are introduced and old batches are removed.

The fixed-enrichment search and enrichment search options of REBUS-3 were used to arrive at equilibrium fuel cycles for the four scenarios developed in this study. "Enrichment search" was the method of performing equilibrium fuel cycle calculation using REBUS-3 used for scenarios A and D. In an enrichment search, the search identifies the fuel loading that is necessary to achieve the desired equilibrium fuel cycle parameters of thermal

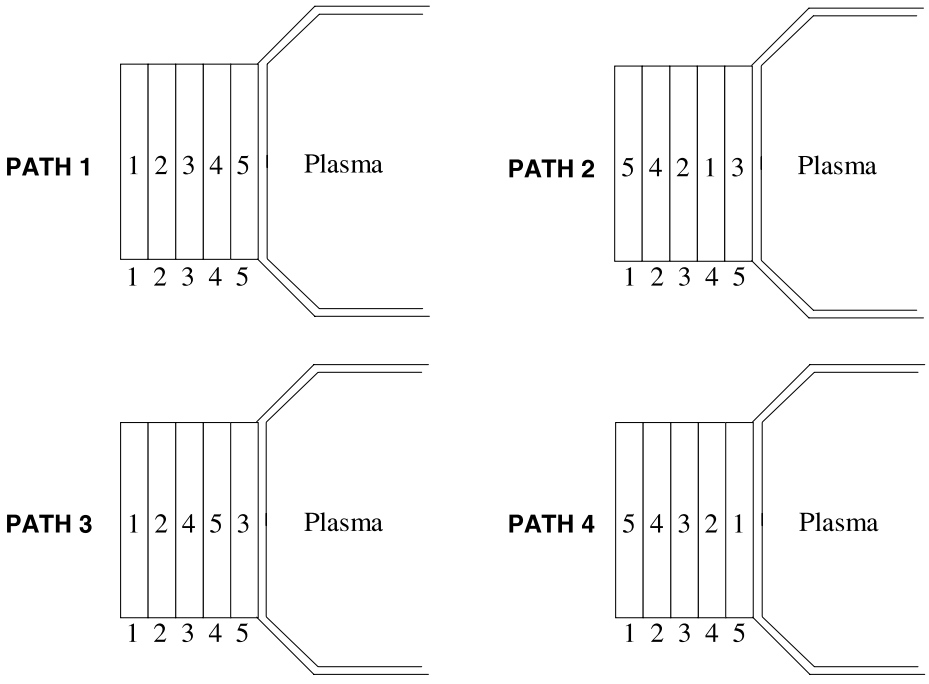

Fig. 2. Fuel paths.

power, k_{eff}^{BOC}, and cycle time. REBUS-3 performs an iterative search until it converges on the equilibrium fuel cycle within the specified k_{eff}^{BOC} tolerance and reports the fraction of TRUs the user has allocated to the core that is required to meet the chosen performance characteristics. Based on these results, the user will increase or decrease the fuel volume fraction, as the case may be, and run another case until the desired enrichment is achieved. A tolerance of <1% of TRU enrichment was used.

"Fixed-enrichment search" was used to determine the equilibrium fuel cycles for scenarios B and C. The equilibrium fuel cycle is found for the given fuel cycle parameters of thermal power, fresh feed composition, and cycle time.

TABLE III

Summary of Scenarios

Scenario	Description
Scenario A	Fuel reprocessed, BOC $k_{eff} = 0.95$, EOC $P_{fus} < 200$ MW
Scenario B	Fuel reprocessed, BOC $k_{eff} < 0.95$, EOC $P_{fus} < 200$ MW
Scenario C	Fuel not reprocessed, BOC $k_{eff} < 0.95$, no restriction on EOC P_{fus}
Scenario D	Fuel recycled without reprocessing, BOC $k_{eff} < 0.95$, EOC $P_{fus} < 200$ MW

IV. FUEL CYCLE SCENARIOS

The primary objective is to achieve >90% burnup of the TRU fuel. The secondary objective is to do this without having to reprocess the TRISO particles. How these objectives can be met depends primarily on the limits placed on k_{eff}^{BOC} and P_{fusion}^{EOC}. The four scenarios in this study explore the effect of changing the restrictions placed on k_{eff}^{BOC} and P_{fusion}^{EOC} with respect to achieving the primary and secondary design objectives.

In scenario A, the k_{eff}^{BOC} is restricted to 0.95, the P_{fusion}^{EOC} is restricted to <200 MW, and reprocessing is performed after each five-batch burn cycle for a given batch of fuel. In scenario B, the k_{eff}^{BOC} is allowed to be <0.95, the P_{fusion}^{EOC} is restricted to <200 MW, and reprocessing is performed. The reprocessing of scenarios A and B is with the following assumptions: (a) constant TRU isotopic composition during irradiation and (b) perfect extraction of the TRUs during reprocessing. In scenario C, the k_{eff}^{BOC} is allowed to be <0.95, no restrictions are placed on P_{fusion}^{EOC}, and a single-pass fuel cycle is used. In scenario D, the k_{eff}^{BOC} is allowed to be <0.95, the P_{fusion}^{EOC} is restricted to <200 MW, and reprocessing is not performed.

A summary of the scenarios is given in Table III.

The requirement that the core must have a k_{eff}^{BOC} of 0.95 (imposed to ensure a safe margin to prompt criticality) is a restriction on core reactivity. This is effectively a restriction on the TRU mass in the core because the reactivity depends on the TRU mass ($k_{eff}^{BOC} \Rightarrow M_{TRU}^{core,BOC}$). A deeper burn will result in less TRU mass and lower reactivity.

Longer burn times will result in deeper burn, so the k_{eff}^{BOC} restriction is also a restriction on cycle time. Consider the five-batch core of this design. Fuel will debut in one core region, burn there, and then move in succession to the other four core regions. Thus, after a batch has been burned once, it will still be in the core for the next four burn cycles, where it will contribute to the reactivity of the whole core. The more it is burned, the lower this contribution will be.[b] Since the degree of its burn depends on how long it has been burned, the k_{eff}^{BOC} restriction becomes a restriction on cycle time.

When it has burned once in every region (five total burns), it will leave the core and be cooled for a time before it is reprocessed or placed in storage and a new batch will be placed in the region in which the discharged batch debuted. This is a continuing process, so that at EOC, one five-burned batch is discharged, and one fresh batch is inserted into the core. This new batch will compensate for the reactivity losses incurred by the batches remaining in the core, but only up to a point, because only so much fuel will fit in the fuel pins (the maximum practical packing fraction limit of 60%). Once the cycle time is found such that the new batch must have the 60% packing fraction to achieve $k_{eff}^{BOC} = 0.95$, the amount of burnup that can be achieved in a single pass through the core has been maximized. Increasing the cycle time any more will increase the single-pass burnup but will also necessarily decrease the k_{eff}^{BOC} below 0.95. Thus, a restriction on k_{eff}^{BOC} is effectively a limit on the cycle time and thus on the cumulative burnup a given batch will experience in a single pass through the core.

The requirement that the core must have a $P_{fusion}^{EOC} <$ 200 MW (P_{fusion}^{EOC} limit of GCFTR-2), like the k_{eff}^{BOC} restriction, is also a restriction on core reactivity ($P_{fusion}^{EOC} \Rightarrow k_{eff}^{EOC} \Rightarrow M_{TRU}^{core,EOC}$) and thus limits the burnup by limiting cycle time ($k_{eff}^{BOC} - k_{eff}^{EOC} \Rightarrow M_{TRU}^{core,BOC} - M_{TRU}^{core,EOC} = \Delta M_{TRU}^{core} \Rightarrow cycle\ length$). The fusion neutron source supplements the neutron population of the reactor core such that the fission power of 3000 MW(thermal) can be constantly maintained, $P_{fis} = \text{const} \cdot \ell P_{fus}/(1 - k_{eff})$, where ℓ is the neutron lifetime. As the burnup increases over a burn cycle, the fusion power must be increased. Thus, a larger burnup will require a larger fusion power, and the 200-MW limit on source strength becomes a limit on the burnup and cycle time.

[b] It should also be noted that no fertile material is present in the fuel, which would also serve to compensate for reactivity losses because it would generate new fissile material via neutron capture and decay.

It was found that the $k_{eff}^{BOC} = 0.95$ restriction resulted in a $P_{fusion}^{EOC} \approx 95$ MW, automatically satisfying the $P_{fusion}^{EOC} < 200$ MW restriction.

These restrictions on core reactivity do not prevent the primary objective from being achieved as long as (a) recycling is possible (if the burnup is <90%) or (b) 90% burn is achieved in a single pass through the core (five-batch burn).

It is not possible to achieve 90% burn in a single pass in GCFTR while maintaining a k_{eff}^{BOC} of 0.95 because the deep burn lowers the core TRU mass too much. For the same reason, it is not possible to achieve 90% burn in a single pass if k_{eff}^{BOC} is allowed to be <0.95 while maintaining the $P_{fusion}^{EOC} < 200$ MW. Thus, it is necessary to consider recycling. Since the k_{eff}^{BOC} and P_{fusion}^{EOC} restrictions are limits on core reactivity, they determine what type of recycling is possible, i.e.,

type 1: recycling with reprocessing

type 2: recycling without reprocessing.

The restrictions determine the type of recycling because the two types differ in the reactivity of the recycle streams. Type 1 recycling has a more reactive recycle stream than type 2 since type 2 will contain fission products that act as parasitic absorbers and depleted fuel.

In type 1 recycling the TRISO fuel discharged from the reactor is taken apart, and the kernels are separated into fission products and the remaining TRUs. The fission products are sent to an HLWR, and the unburned TRUs join the mixture of TRUs from processing of LWR SNF. This combination of fresh TRUs from LWR SNF and unburned TRUs from irradiated TRISOs is used to form new TRISO particles that will be fabricated into fuel pins and burned again in the reactor.

In type 2 recycling the fuel discharged from the reactor is not reprocessed; thus, the fission products that accumulate during irradiation will remain with the depleted fuel. The burned fuel is mixed with newly fabricated fuel. The mixture of burned pins and new pins is burned in the reactor.

Achievement of the secondary objective requires the use of type 2 recycling only. This was found to be impossible with $k_{eff}^{BOC} = 0.95$ and $P_{fusion}^{EOC} < 200$ MW and very inefficient with $k_{eff}^{BOC} < 0.95$ and $P_{fusion}^{EOC} < 200$ MW. Thus, type 1 recycling with reprocessing was also considered.

Scenario A was the first fuel cycle explored in this study. It is a recycling fuel cycle with reprocessing in which both the k_{eff}^{BOC} and P_{fusion}^{EOC} restrictions are enforced. Four versions of scenario A were evaluated, each with a different fuel path, with the purpose of evaluating burnup as a function of fuel path.

Scenario B arose from the observation that for scenario A, the P_{fusion}^{EOC} was ~95 MW, far short of the 200-MW limit. The more restrictive $k_{eff}^{BOC} = 0.95$ restriction was removed to increase the burnup per five-batch burn by increasing the cycle time and thus reducing the number of passes required to achieve 90% burn. Scenario B, like scenario A, is a recycling case with reprocessing.

In scenario C, the $k_{eff}^{BOC} = 0.95$ constraint was relaxed, and the fusion power was increased to the level necessary to achieve 90% burn in just one pass (no recycle necessary).

In scenario D, recycling without reprocessing was explored to achieve the secondary objective. It is similar to scenario B in that the k_{eff}^{BOC} was allowed to be <0.95 while the P_{fusion}^{EOC} was restricted to <200 MW. It is different from the other three scenarios in that the input feed is a mixture of two feed streams of different composition: (a) low-reactivity recycled fuel from previous reactor discharges and (b) high-reactivity fresh fuel from LWR SNF. Fuel that is discharged from the reactor at the end of a burn cycle is sent back through the reactor continuously, completely destroying the TRU content of the fuel. Since reprocessing is not employed, the fission products are retained and build up over the duration of the burn and constitute a parasitic absorber. The changing composition of the TRU fuel also tends toward a less reactive isotopic composition as irradiation continues (see Sec. V.E). Thus, the recycled fuel becomes increasingly less reactive as irradiation continues. This makes it necessary to supplement the core loading of each batch with fresh feed, i.e., new TRISOs that have been created from LWR SNF.

The two feed streams are mixed such that as much of the recycle stream as possible is used in the new core charge. When this new batch has itself burned five times, i.e., completed a single pass, it will be discharged to the recycle stream, where it mixes homogeneously with the rest of the discharged fuel. This recycle feed is combined with more fresh fuel for another charge.

Scenario D was evaluated at a cycle time of 330 days to maximize the fraction of the feed stream composed of recycled fuel. Because it imposes the least restrictive requirements on reactivity within the design constraints, 330 days maximizes the recycle fraction. It should be recalled from the discussion on the relationship between k_{eff}^{BOC} and cycle time that the longer the cycle time, the lower the equilibrium core reactivity. Setting the cycle time at 330 days will thus minimize the required equilibrium core reactivity and maximize the amount of recycled fuel in the reactor feed.

The recycle stream will consist of fuel of a variety of burnups since it will be a combination of the discharge of every stage in the fuel cycle. Ideally, the recycled TRISOs would be removed from the fuel cycle once 90% burnup of the TRUs is reached and would be sent to an HLWR. In the recycling fuel cycle modeled here, however, the fuel never leaves the fuel cycle, which means the recycle stream will be less reactive than in the ideal case. So, scenario D constitutes a conservative estimate to a recycling fuel cycle in which fuel is removed at 90% burn.

Design constraints in addition to those on k_{eff}^{BOC} and P_{fusion}^{EOC} were enforced in all scenarios. Power peaking was limited to below 2 for safety reasons. The packing fraction was limited to 60%. The tritium inventory produced during a given cycle was designed to last for a between-cycle downtime of at least 90 days to ensure an adequate supply. It was also desired, but not enforced, that the cycle time exceed 330 days to ensure reasonable availability.

V. TRANSMUTATION PERFORMANCE

V.A. Scenario A

The results (Table IV) indicate that the primary objective of >90% TRU burnup can be achieved by all paths, and destruction of the TRUs would be achieved at a rate of 1.12 tonnes/full-power year (FPY) of TRUs. This corresponds to an SNF disposal per year of 100 tonnes.

The "LWR support ratio" refers to the ratio of TRUs destroyed by a given reactor to TRUs produced by a 1000-MW(electric) LWR in 1 FPY. Since a typical 1000-MW(electric) LWR will produce ~360 kg FPY of TRUs (Ref. 14) as compared to 1.12 tonnes/FPY destroyed by a GCFTR-2, the support ratio is 3 for all paths.

The 330-day cycle time goal was not achieved for any path. Since the fuel in this scenario is the most optimistic with respect to recycled feed reactivity (recall assumptions in Sec. IV) and it still cannot attain 330 days, type 2 recycling without reprocessing certainly cannot be achieved with this scenario. Fuel recycled without reprocessing will be reduced in TRU content and will contain fission products, which act as parasitic absorbers, resulting in a much less reactive composition. Less

TABLE IV

Scenario A Results

Parameter	Path 1	Path 2	Path 3	Path 4
Cycle length (days)	280	305	240	260
Five-batch residence (yr)	3.83	4.18	3.29	3.56
Packing fraction (%)	60	60	60	60
BOC k_{eff}	0.951	0.949	0.950	0.951
EOC k_{eff}	0.924	0.919	0.928	0.927
BOC P_{fus} (MW)	38.7	39.3	39.7	38.5
EOC P_{fus} (MW)	91.3	94.7	82.4	90.5
Lithium fraction in reflector[a] (%)	4.07	4.50	3.65	4.35
Tritium burned/cycle (kg)	2.74	3.07	2.21	2.53
Tritium produced/cycle (kg)	2.83	3.17	2.28	2.64
Tritium intercycle downtime (days)	90	90	90	90
Tritium lead time (days)	180	185	162	222
BOC power peaking	1.70	1.83	1.63	1.73
EOC power peaking	1.52	1.71	1.47	1.62
TRU BOC load (tonne)	35.3	34.6	35.3	34.9
TRU EOC load (tonne)	34.4	33.7	34.6	34.1
TRU burned/core/year (tonne/FPY)	1.12	1.12	1.11	1.12
TRU burn/residence (%)	11.6	12.7	10.0	10.8
LWR support ratio[b]	3	3	3	3
SNF disposed per year (tonne/FPY)	100	100	100	100
Average cycle flux (n/cm^2·s)	5.62E+14[d]	5.66E+14	5.59E+14	5.60E+14
Average cycle fast flux[c] (n/cm^2·s)	2.33E+14	2.34E+14	2.31E+14	2.32E+14
Fluence/residence (n/cm^2)	6.80E+22	7.45E+22	5.79E+22	6.29E+22
Fast fluence/residence (n/cm^2)	2.81E+22	3.08E+22	2.40E+22	2.61E+22
Core passes for 90% burn	19	17	22	21
Total residence for 90% burn (yr)	73	71	72	75
Fluence at 90% burn (n/cm^2)	1.29E+24	1.27E+24	1.27E+24	1.32E+24
Fast fluence at 90% burn (n/cm^2)	5.35E+23	5.24E+23	5.28E+23	5.48E+23

[a]Only applies to inner, outer, and central reflectors. The upper reflector contains no lithium.
[b]Assuming 360 kg/FPY of TRUs produced.[14]
[c]Fast flux is >0.11 MeV.
[d]Read as 5.62×10^{14}.

reactive fuel, in turn, will result in lower cycle times. For this reason, type 2 recycling cases with $k_{eff}^{BOC} = 0.95$ could not be achieved for this design.

The TRU burn/residence was calculated as a simple mass balance of the TRU isotopes present in the fresh fuel over an equilibrium cycle (isotopes of Table II). TRU burn/residence ranged from 10 to 12.7%. This is also referred to as the single-pass burn.

The $P_{fusion}^{EOC} < 200$ MW requirement is satisfied as a consequence of the k_{eff}^{BOC} constraint. This is because the cycle times necessary to achieve $k_{eff}^{BOC} = 0.95$ all corresponded to P_{fusion}^{EOC} values of 90 to 95 MW.

The average cycle fluxes and fast fluxes, though not equal, are all very close to one another. Since the cycle times vary from path to path, however, the fluence also varies, with the highest seen in the paths with the longest cycle times. The P_{fusion}^{EOC} also follows this trend since longer cycle times make for deeper burn, requiring greater compensation from the neutron source to maintain the power level. Thus, the ranking of P_{fusion}^{EOC} from highest to lowest corresponds to the ranking of cycle times from longest to shortest. In consequence of this, the tritium consumption follows the same trend since tritium is the fuel for the fusion neutron source.

All cases operated with power profiles sufficient to maintain the power peaking below the design goal of 2. We note that none of the standard methods to reduce power peaking (fuel zoning within assemblies, burnable poisons, etc.) have been employed in these first fuel cycle analyses of the GCFTR, so the power peaking numbers given in Table IV should be interpreted as conservative upper limits.

The neutron flux energy distribution varied only slightly among the four paths, so path 1 was taken to be representative of them all. As shown in Fig. 3, almost the entire flux is contained in the range from 100 eV to 10 MeV.

Note that a calculation error in the previous GCFTR studies[24,25] was corrected in this analysis. The fuel cycle results in Ref. 25 should be replaced with those of scenario A, path 1 of this analysis.

Path 1

Path 1 consists of a simple out-to-in shuffle pattern. The fuel cycle time was limited to 280 days as a consequence of the k_{eff}^{BOC} restriction of 0.95. A greater cycle time could have been achieved were it possible to increase the TRU volume fraction of the core, but this is not possible considering that the TRISO packing fraction is already maximal at 60%. This 280-day cycle time results in an 11.6% burnup of the initial TRU content per pass through the reactor.

The average BOC and EOC axially averaged radial power distributions are shown in Fig. 4 for path 1. The low power densities are a consequence of REBUS-3 performing the power calculations over the whole volume of the specified subregion as opposed to just over the volume of the fuel. Thus, the figures are meant to show relative power distributions rather than absolute power levels.

Path 2

In path 2, the fuel follows a path from highest flux region to lowest flux region in an effort to increase the cycle time such that a greater availability could be achieved (target > 330 days). The intent of this case is to maximize

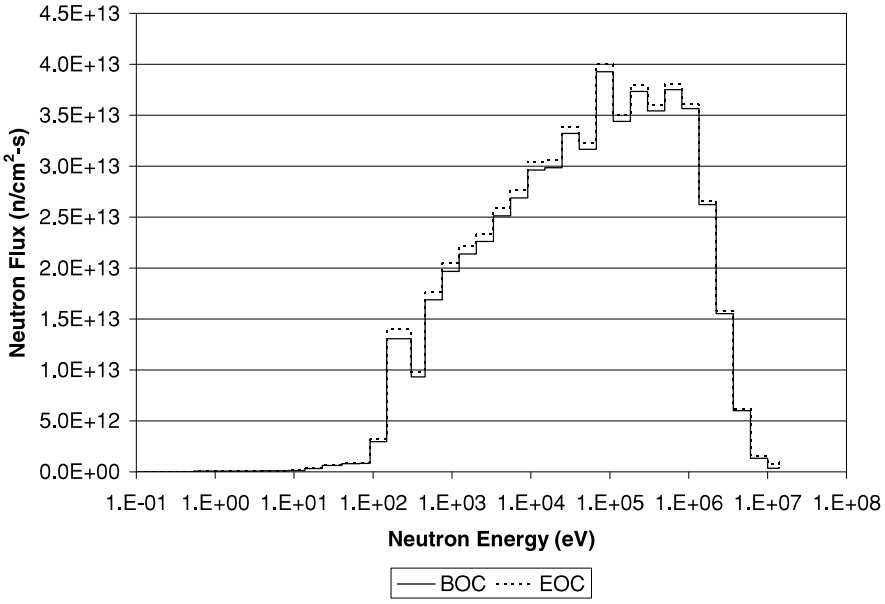

Fig. 3. Scenario A flux spectrum.

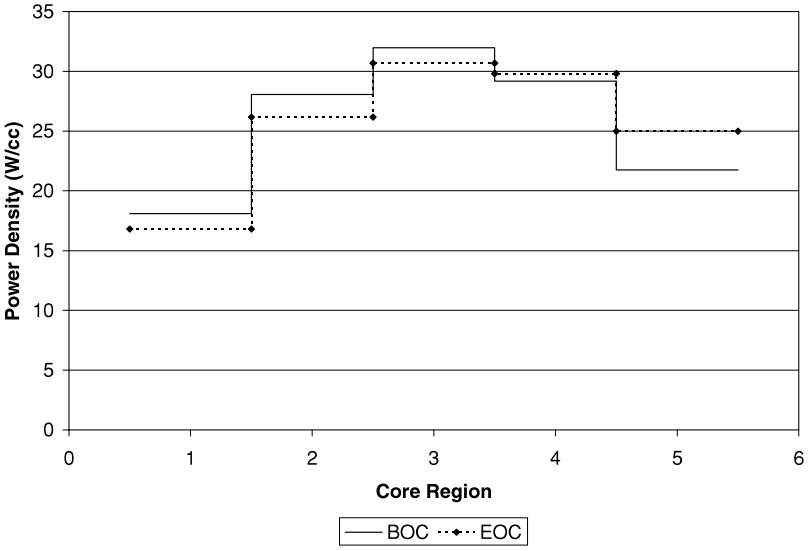

Fig. 4. Path 1 power distribution.

cycle time by keeping the most reactive fuel in the regions that naturally have the highest flux. In a typical reactor, the power profile would be similar to a cosine, peaking in the center and symmetric in the radial direction. This reactor, however, is asymmetric because of a source on the inboard side, which shifts the peak power and flux into region 4. The substantial shift of power (and thus flux) toward the plasma is distinct at BOC and even more so at EOC.

Averaging BOC and EOC power densities in each subregion, we can rank the core regions' highest average power to lowest average power as follows: 4, 3, 5, 2, and 1. The fuel for path 2 follows this same sequence, debuting in the reactor in region 4; moving through 3, 5, and 2; and finally burning in region 1. As one would expect, this case has the highest power peaking (but is still under the design limit of 2). It also achieves the highest cycle time (305 days), as was the intent, though is still shy of the 330-day goal. The power profile, relative to path 1, shifts rightward, peaking in region 4 at BOC and EOC.

Path 3

In path 3, the fuel follows a path from the lowest flux region to the highest flux region (the converse of path 2) in an effort to flatten the power profile and minimize the peaking. The power profile is essentially the same as that of path 1 (Fig. 3). It has the shortest cycle time (240 days), highest k_{eff}^{EOC}, lowest tritium burn, lowest lithium volume fraction in the reflectors, and lowest $P_{fusion}^{\mathrm{EOC}}$. It also has the lowest power peaking of the four paths.

Path 4

Path 4 is the converse of path 1. Path 4 has a slightly lower BOC core loading and higher power peaking relative to path 1 due to the proximity of fresh fuel to the flux peak. Its power profile is similar to that of path 2.

V.B. Scenario B

See Table V for the results of this fuel cycle. The k_{eff}^{BOC} was 0.930, and EOC was 0.900. The $P_{fusion}^{\mathrm{EOC}}$ was 199 MW. The larger fusion power relative to scenario A results in a much larger requirement for the tritium inventory and reflector lithium volume fraction. As was expected, relaxing the k_{eff}^{BOC} constraint resulted in a longer fuel cycle (376 versus 280 days) for the chosen fuel path achieving the availability goal of >330-day cycle time. The longer cycle time results in a larger single-pass burnup (15.3% was achieved versus 11.6% achieved by path 1 of scenario A) but still much less than 90%. The TRU destruction rate is 1.13 tonnes/FPY.

The flux spectrum is almost identical to scenario A except for a slightly more energetic spectrum and a slightly larger flux, particularly at EOC. This is due to the larger burnup caused by a longer cycle time, which necessitates a larger flux from the neutron source. This increases the fraction of the core neutron population composed of the more energetic fusion neutrons.

V.C. Scenario C

See Table V for the results. The single-pass equilibrium burn was 90.0% with a cycle time of 3000 days. After 41 yr of irradiation, 90% burn would be achieved. The fusion power necessary to achieve this burnup was 1803 MW at BOC and 3366 at EOC, which is not possible for the GCFTR neutron source as designed, and these results are shown purely for illustrative purposes. The fast fluence at 90% burnup is 6.45×10^{23} n/cm^2. Tritium self-sufficiency was nearly achieved with 76.3%

TABLE V

Scenarios B, C, and D Results

Parameter	B	C	D
Cycle length (days)	376	3000	330
Five-batch residence (yr)	5.15	41.07	4.52
Packing fraction (%)	60	60	60
BOC k_{eff}	0.936	0.383	0.860
EOC k_{eff}	0.900	0.127	0.827
BOC P_{fus} (MW)	122.1	1803	120.0
EOC P_{fus} (MW)	199.1	3366	187.5
Lithium fraction in reflector (%)	28.00	100.00	25.00
Tritium burned/cycle (kg)	9.02	975	7.61
Tritium produced/cycle (kg)	9.34	756	7.82
Tritium lead time (days)	200	—	162
Tritium intercycle downtime (days)	90	—	90
BOC power peaking	1.73	1.49	1.73
EOC power peaking	1.53	1.34	1.54
TRU BOC load (tonne)	34.9	24.2	34.9
TRU EOC load (tonne)	33.8	17.9	33.9
TRU burned/core/year (tonne/FPY)	1.10	0.81	1.11
TRU burn/residence (%)	15.3	90.0	13.7
LWR support ratio	3	2	3
SNF disposed per year (tonne/FPY)	98	73	99
Average cycle flux (n/cm^2·s)	5.78E+14[a]	1.17E+15	5.76E+14
Average cycle fast flux (n/cm^2·s)	2.42E+14	4.97E+14	2.42E+14
Fluence/residence (n/cm^2)	9.39E+22	1.52E+24	8.22E+22
Fast fluence/residence (n/cm^2)	3.94E+22	6.45E+23	3.45E+22
Core passes for 90% burn	14	1	16
Total residence for 90% burn (yr)	72	41	72
Fluence at 90% burn (n/cm^2)	1.31E+24	1.52E+24	1.31E+24
Fast fluence at 90% burn (n/cm^2)	5.51E+23	6.45E+23	5.52E+23

[a]Read as 5.78×10^{14}.

of the required tritium produced. This required the entire volume of all the reflector regions to be composed of Li_2O, including the upper reflector.

The flux distribution is depicted in Fig. 5. It indicates a much larger average core flux, particularly at EOC. The average core flux and average core fast flux are double that of the other three scenarios. This is due to the very high burnup of this core, which requires a much larger fusion power level to maintain the fission power level.

As a consequence of the high lithium concentration in the reflector and the larger core flux, the exothermic reaction ($^6Li + n \rightarrow {}^4He + T + energy$) contributes a much larger amount of the reactor power than in the other scenarios. As a result, fewer TRUs need to be fissioned to maintain the power level, so the TRU destruction rate (0.81 tonnes/FPY) is lower than the other scenarios. The fraction of the total power that comes from the core is 81% at BOC and 67% at EOC, the balance coming primarily from exothermic reactions in the reflectors. For the other scenarios, the TRU destruction rate is 1.12 tonnes/FPY, and ~97% of the reactor power is generated in the core with little variation from BOC to EOC.

The large demands placed on the fusion neutron source indicate that near-term deployment of such a reactor is not feasible and that recycling scenarios with reprocessing are the only means to 90% burn of the TRU fuel at the present time.

V.D. Scenario D

See Table V for the results. Scenario D is an equilibrium fuel cycle with the maximum amount of fuel that can be recycled without reprocessing to achieve 90% burnup in a burn cycle with a 330-day length, $k_{eff}^{BOC} < 0.95$, and $P_{fusion}^{EOC} < 200$ MW. Scenario D was the only scenario to meet both the primary (>90% burnup) and secondary (without reprocessing) design objectives. It was found that the equilibrium fuel cycle had a k_{eff}^{BOC} of 0.860 and a P_{fusion}^{EOC} of 188 MW. The TRU destruction rate of 1.11 tonnes/FPY and the LWR support ratio of 3 were the same as scenarios A and B. This was achieved by recycling only a small amount of burned TRU fuel with a large amount of fresh TRU from SNF. The recycled feed fraction was 6.2% (by mass). This is not a very large

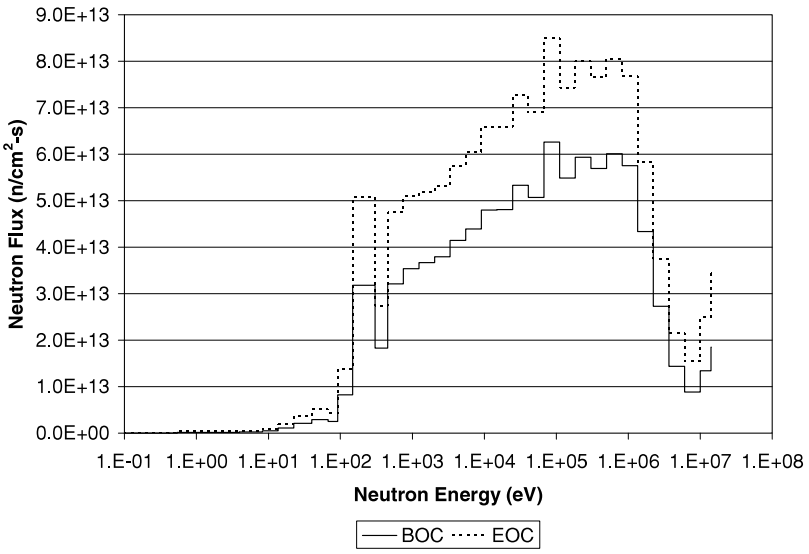

Fig. 5. Scenario C flux spectrum.

number but should be regarded as a lower bound considering that the computational model is a conservative estimate of the case in which TRISOs are removed after they achieve 90% burn. This scenario is not practical because of the implied accumulation of five-batch burned TRU fuel but is shown for illustrative purposes.

The flux spectrum is essentially identical to scenario B.

V.E. Isotopic Composition During Irradiation

The relative isotopic distribution of the TRU fuel was calculated at several equally spaced time steps during irradiation to evaluate the reasonableness of the assumption made for the reprocessing cases (scenarios A and B) of constant isotopic distribution among TRU components during irradiation. The results are shown in Fig. 6. Isotopes not shown (^{244}Pu, ^{242m}Am, ^{242}Cm, ^{243}Cm, ^{247}Cm) each account for $<1\%$ for the duration of the burn and are omitted.

Far from being constant, the isotopic distribution changes significantly as irradiation proceeds. The first assumption used for the reprocessing approximations of scenarios A and B is thus incorrect. The predominant change in the distribution is the relative reduction of ^{239}Pu and the relative increase of ^{240}Pu and ^{242}Pu.

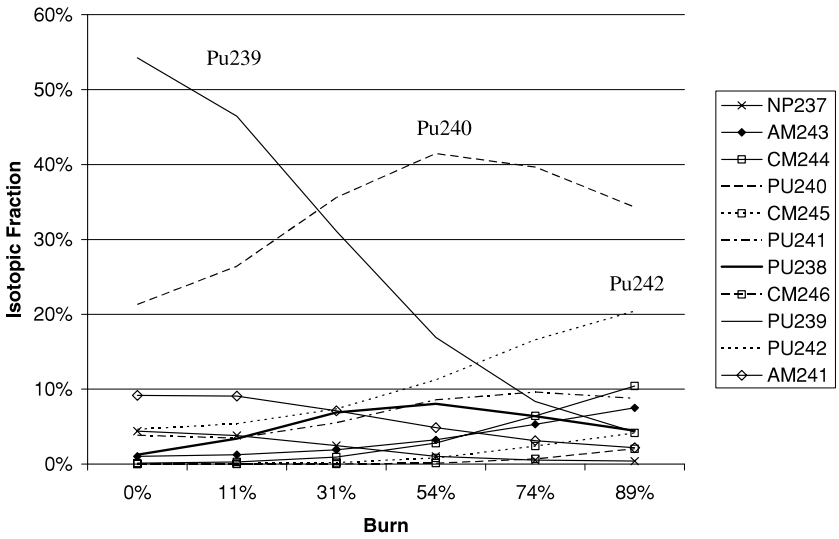

Fig. 6. Isotopic distribution trends.

Plutonium-239 has a smaller capture-to-fission ratio than either ^{240}Pu or ^{242}Pu by a factor of 2 to 3 in a fast spectrum indicating that as the burn proceeds, the isotopic mixture is increasingly less reactive. Curium-244 also increases from <1% to >10% of the isotopic mixture and has a fast capture-to-fission ratio comparable to that of ^{242}Pu. These changes also have to be weighed by the depletion in TRU isotopes because as the burn proceeds, the contribution of a given sample of previously burned TRUs will diminish. The net effect, however, is clearly toward less reactivity than in the constant-isotopic-distribution assumption, with the implication of even shorter cycle lengths than calculated above, and hence even greater difficulty in obtaining deep burn without reprocessing.

VI. SUMMARY AND CONCLUSIONS

A fuel cycle analysis for a subcritical gas-cooled fast reactor [GCFTR-2 (Ref. 25)] with the primary objective of achieving >90% burn of the TRU TRISO fuel was evaluated, and the possibility of achieving this burnup without reprocessing the TRISO particles was investigated.

In principle, essentially total destruction of the TRUs could be achieved in the 3000-MW(thermal) GCFTR at the rate of ~1.12 tonnes/FPY for all fuel cycles considered, except for the single-pass fuel cycle. This transmutation rate corresponds to the disposal of ~100 tonnes/FPY of SNF. A single such 3000-MW(thermal) GCFTR could support, i.e., burn, the TRU in the SNF from three 1000-MW(electric) LWRs, and a fleet of 35 GCFTRs could support the entire U.S. nuclear reactor fleet at current levels of power production.

However, the analysis of this paper indicates that repeated reprocessing of the TRISO fuel to remove the fission products and replenish the depleted TRUs is necessary to achieve burnups greater than ~13%, with pure TRU fuel and D-T fusion neutron sources operating at the 200-MW level. A reprocessing scheme, based on first grinding the TRISO particles into 100-μm pieces and then employing a series of uranium extraction/TRU extraction processes was developed and judged to be feasible but unattractive because of the large mass of nonfuel material involved.[26]

The burn cycles varied from 240 to 305 days, which is probably a little short for practicality. Achievement of 90% TRU burnup would require multiple passes of the reprocessed fuel (as many as 22) through the reactor. A relatively low single-pass burnup, multiple passes through the core, and reprocessing to remove fission products are all consequences of maintaining a high level of reactivity in the core such that operation can occur with a $k_{eff}^{BOC} = 0.95$ and at a modest fusion neutron source strength of $P_{fusion}^{EOC} < 200$ MW (scenario A).

Several other possible fuel cycles were evaluated by relaxing the constraints on k_{eff}^{BOC} and P_{fusion}^{EOC} to provide perspective. By relaxing only the $k_{eff}^{BOC} = 0.95$ constraint (scenario B) but maintaining the $P_{fusion}^{EOC} \leq 200$ MW constraint on the fusion neutron source strength, the five-batch fuel cycle burnup was increased to ~15% per pass, and the cycle time was increased to 376 days, but multiple reprocessing and recycling steps would still be required to achieve >90% TRU burnup. This fuel cycle seems practical, assuming the practicality of reprocessing the TRISO fuel.

By relaxing both $k_{eff}^{BOC} = 0.95$ and $P_{fusion}^{EOC} \leq 200$ MW, a deep burn of 90% could be achieved in a single five-batch cycle of 41-yr duration without reprocessing but required a P_{fusion}^{EOC} of ~3400 MW (scenario C), which is well beyond the capability of the GCFTR fusion neutron source (or near-term fusion neutron sources in general).

Relaxing the BOC requirement (to $k_{eff}^{BOC} = 0.86$) and maintaining the EOC $P_{fusion}^{EOC} \leq 200$ MW requirement, but maintaining the reactivity level by charging the reactor at the beginning of each burn cycle with only 6% recycled fuel plus 94% fresh TRU fuel (scenario D), enabled the GCFTR to achieve 330-day burn cycles and >90% TRU burnup without reprocessing; however, such a fuel cycle is probably impractical and is only discussed to provide perspective.

The GCFTR could be self-sufficient in tritium production for all these fuel cycles, with the exception of the high fusion power scenario C in which 76% of the tritium required was produced. The GCFTR could be redesigned for tritium self-sufficiency in this fuel cycle, but as mentioned the fuel cycle is not of near-term interest.

The above results of the fuel cycle analysis suggest that to achieve the objectives of deep burn of TRU without reprocessing, the design of the GCFTR should be changed either (a) to allow for a stronger neutron source to compensate a greater negative reactivity accumulation [$P_{fis} = \text{const} \cdot \ell P_{fus}/(1 - k_{eff})$] or (b) ^{238}U should be admixed with the TRU fuel to create fresh TRU fuel in situ to offset the negative reactivity decrement of TRU depletion and fission product buildup—or both. The second option would be inconsistent with a purely deep-burn transmutation goal for GCFTR but would be consistent with the somewhat broader goal of more effective utilization of the uranium mined for nuclear fuel (including extraction of energy from the TRU in SNF).

The GCFTR concept of deep burn without reprocessing depends critically on the extended lifetime of the TRISO fuel particle in a fast neutron environment, a matter that remains to be demonstrated. McEachern[31] indicates that fast fluences on the order of 4×10^{21} to 8×10^{21} n/cm^2 are limiting for TRISO particles in a fast spectrum, which is a value exceeded by even the lowest burnup case of this study (10.0%). However, this estimated fluence limit is for the nominal TRISO particle designed for use in a thermal spectrum reactor. In the GCFTR-2 design the conventional TRISO design was

modified by reducing the kernel and enlarging the buffer region in anticipation of fast fluence limitations,[32] and the ability to withstand the fission product gas buildup was calculated.[25,26]

Finally, the need to compare the transmutation, or more generally the TRU management, performance of subcritical, TRISO-fueled GCFTRs with the performance of more conventional, critical gas-cooled fast reactors that can burn comparable annual amounts of TRU (e.g., Ref. 32) is noted. While the detailed comparison needed is beyond the scope of this initial paper exploring the types of fuel cycles accessible to the GCFTR, two general comments can be made. First, the ability to operate subcritical with highly burned fuel offers a broader choice of fuel cycles, subject to the ability of the fuel to sustain deep burnup without failure due to radiation damage, which provides a greater flexibility for fuel management, resource utilization, and reduction of waste that must be stored in geological repositories. Second, the larger margin to prompt criticality provided by subcritical operation should allow for higher TRU loadings and hence higher net transmutation rates. Whether these advantages can offset the added cost and complexity of a subcritical system with an integrated neutron source remains to be seen.

REFERENCES

1. "A Roadmap for Developing Accelerator Transmutation of Waste (ATW) Technology," DOE/RW0-519, U.S. Department of Energy (1999).

2. E. A. HOFFMAN and W. M. STACEY, "Comparative Fuel Cycle Analysis of Critical and Subcritical Fast Reactor Transmutation Systems," *Nucl. Technol.*, **144**, 83 (2003).

3. W. M. STACEY, *Nuclear Reactor Physics*. John Wiley & Sons, Inc., New York (2001).

4. "First Phase P&T Systems Study: Status and Assessment Report on Actinide and Fission Product Partitioning and Transmutation," Organization for Economic Cooperation and Development/Nuclear Energy Agency (1999).

5. *Proc. 1st through 5th NEA International Exchange Mtgs.*, Paris, France, Organization for Economic Cooperation and Development/Nuclear Energy Agency (1990 through 1998).

6. "Nuclear Wastes—Technologies for Separations and Transmutations," National Research Council, National Academy Press (1996).

7. C. D. BOWMAN et al., "Nuclear Energy Generation and Waste Transmutation Using Accelerator-Driven Intense Thermal Neutron Source," *Nucl. Instrum. Methods A*, **320**, 336 (1992).

8. W. C. SAILOR et al., "Comparison of Accelerator-Based with Reactor-Based Nuclear Waste Transmutation Schemes," *Prog. Nucl. Energy*, **28**, 359 (1994).

9. T. A. PARISH and J. W. DAVIDSON, "Reduction in the Toxicity of Fission Product Wastes Through Transmutation with Deuterium-Tritium Fusion Neutrons," *Nucl. Technol.*, **47**, 324 (1980).

10. E. T. CHENG et al., "Actinide Transmutation with Small Tokamak Fusion Reactors," *Proc. Int. Topl. Conf. Evaluation of Fuel Cycle for Future Nuclear Systems (Global '95)*, Versailles, France, 1995 (1995).

11. Y.-K. M. PENG and E. T. CHENG, "Magnetic Fusion Driven Transmutation of Nuclear Wastes (FTW)," *J. Fusion Energy*, **12**, 381 (1993).

12. E. T. CHENG and R. J. CERBONE, "Prospect of Nuclear Waste Transmutation and Power Production in Fusion Reactors," *Fusion Technol.*, **30**, 1654 (1996).

13. Y. GOHAR, "Fusion Option to Dispose of Spent Nuclear Fuel and Transuranic Elements," ANL/TD/TM00-09, Argonne National Laboratory (2000).

14. L. J. QIU et al., "A Low Aspect Ratio Tokamak Transmutation System," *Nucl. Fusion*, **40**, 629 (2000).

15. W. M. STACEY, "Capabilities of a DT Tokamak Fusion Neutron Source for Driving a Spent Nuclear Fuel Transmutation Reactor," *Nucl. Fusion*, **41**, 135 (2001).

16. "Non-Electric Applications of Fusion," Final Report to FESAC, Fusion Energy Sciences Advisory Committee (July 31, 2003).

17. W. M. STACEY, "Transmutation Missions for Fusion Neutron Sources," *Fusion Eng. Des.* (to be published).

18. W. M. STACEY, J. MANDREKAS, and E. A. HOFFMAN, "Sub-Critical Transmutation Reactors with Tokamak Fusion Neutron Sources," *Fusion Sci. Technol.*, **47**, 1210 (2005).

19. W. M. STACEY et al. "A Fusion Transmutation of Waste Reactor," *Fusion Sci. Technol.*, **41**, 116 (2002).

20. D. L. JASSBY and J. A. SCHMIDT, "Electrical Energy Requirements for Accelerator and Fusion Neutrons," *Fusion Sci. Technol.*, **40**, 52 (2001).

21. M. P. LaBAR, "The Gas Turbine—Modular Helium Reactor: A Promising Option for Near Term Deployment," GA-A23952, General Atomics (Apr. 2002).

22. C. RODRIGUEZ, A. BAXTER, D. McEACHERN, M. FIKANI, and F. VENNERI, "Deep-Burn: Making Nuclear Waste Transmutation Practical," *Nucl. Eng. Des.*, **222**, 299 (2003).

23. D. A. PETTI, J. BUONGIORNO, J. T. MAKI, R. R. HOBBINS, and G. K. MILLER, "Key Differences in the Fabrication, Irradiation and High Temperature Accident Testing of U.S. and German TRISO-Coated Particle Fuel, and Their Implications on Fuel Performance," *Nucl. Eng. Des.*, **222**, 281 (2003).

24. W. M. STACEY et al., "A Subcritical, Gas-Cooled, Fast Transmutation Reactor with a Fusion Neutron Source," *Nucl. Technol.*, **150**, 162 (2005).

25. W. M. STACEY et al., "A Subcritical, Helium-Cooled Fast Reactor for the Transmutation of Spent Nuclear Fuel," *Nucl. Technol.*, **156**, 99 (2006).

26. W. M. STACEY et al., "Advances in the Sub-Critical, Gas-Cooled, Fast Transmutation Reactor Concept," *Nucl. Technol.*, (accepted for publication).

27. J. W. MADDOX, "Fuel Cycle Optimization of a Helium-Cooled, Sub-Critical, Fast Transmutation of Waste Reactor with a Fusion Neutron Source," MSNE Thesis, Georgia Institute of Technology (2006).

28. B. J. TOPPEL, "A User's Guide to the REBUS-3 Fuel Cycle Analysis Capability," ANL-83-2, Argonne National Laboratory (1983).

29. "DANTSYS: A Diffusion Accelerated Neutral Particle Transport Code System," LA-12969-M Manual UC-705, Los Alamos National Laboratory (1997).

30. H. HENRYSON et al., "MC2-2: A Code to Calculate Fast Neutron Spectra and Multigroup Cross Sections," ANL-8144, Argonne National Laboratory report (1976).

31. D. McEACHERN, General Atomics, Personal Communication (2005).

32. T. D. NEWTON and P. J. SMITH, "Flexibility of the Gas Cooled Fast Reactor to Meet the Requirements of the 21st Century," Serco Assurance report; available on the Internet at www.sercoassurance.com/answers/resource/pdfs/gcfr_flexibility.pdf.